Study of the Surface of Ice, Ice/Solid and Ice/Liquid Interfaces with Scanning Force Microscopy

Victor F. Petrenko

Thayer School of Engineering, Dartmouth College, Hanover, New Hampshire 03755

Received: October 11, 1996; In Final Form: June 2, 1997[⊗]

Contact mode of scanning force microscopy (SFM) and force curves (FC) were used to study the morphology of ice surface in air and in liquid decane and the structure and some physical properties of the interfaces between ice and Si and Si_3N_4 cantilever tips in the temperature range from −0.4 to −20 °C. Evidence for a liquid-like layer on the ice surface came from observation of capillary forces that act on cantilever tips. Intensive mass transport along the ice surface was found at $T \geq -14$ °C. The FCs were used to determine the adhesion strength of ice to Si and Si_3N_4 cantilever tips, the corresponding interfacial energies, the thickness of a liquid-like layer, and the density of an electric charge acquired by the tips from the ice surface.

Introduction

In this study we applied SFM to study the morphology of ice surface and some physical properties of ice/solid interfaces. The physical properties of ice/solid interfaces attracted significant interest during last two decades due to the role they play in icing, ice adhesion, and in frozen grounds. Though in the past most of ice−surface experiments have been performed on ice/(water vapor) and ice/(water vapor + air), we will not discuss them here since the structure and properties of these interfaces may differ significantly from those of ice/solid interfaces. For the same reason we will not mention results obtained on ice surface in vacuum at very low temperature (near or below liquid nitrogen temperature). A reader interested in those interfaces is addressed to recent reviewers of such experimental results.[1,2]

Several experimental techniques have been used in the past to study ice/solid interfaces: optical ellipsometry,[3,4] NMR,[5] and Raman spectroscopies,[6] measurements of interfacial electrical conductivity,[7] measurements of adhesion strength,[8] and measurements of the interface viscosity.[5] Various types of solids were tested as substrates: quartz,[5] metals and alloys,[9] graphite,[10] glass,[3,4] silica,[11] polystyrene,[11] Teflon,[5] and other plastics.[12]

It was found that on most of the interfaces a thin liquid or liquid-like layer (LLL) exists at temperature below the ice melting point. In some cases the LLL was detected at temperatures as low as −93 °C.[5] The thickness of the LLL decreases rapidly as temperature decreases. While optical density of the layer was close to one of ordinary water, the layer electrical conductivity, viscosity, and correlation time of water molecules were very distinct from that of both ordinary water and bulk ice.

Several theoretical models were proposed to describe the structure and physical properties of the ice subsurface layer. In a series of papers, Dash and his coauthors used the idea of a possible lowering in the free energy of the system resulting from the formation of a liquid film between the ice and solid, see review paper in ref 1.

Dzyaloshinskii *et al.*[15] showed that a fluid which is less polarizable than its solid phase is attracted to the solid, causing a liquid film to grow at the solid/vapor interface. Elbaum and Schick applied this theory to ice/vapor interface,[16] and Wilen *et al.*[17] applied this idea to several types of ice/solid interfaces. These models usually predict a much thinner layer than was experimentally observed. But in some cases these phenomenological (nonmicroscopic) models were able to explain an absolute magnitude and temperature dependence of the layer thickness. Nevertheless, the main problem that such models faces is that they imply that the LLL is an ordinary water while it is not. Some properties of the LLL differ from those of ordinary super cooled water by orders of magnitude. The properties of water and those of LLL with the largest differences were the electrical conductivity (≥3 orders of magnitude[7]), viscosity (1 order of magnitude[5]), correlation time (2 orders of magnitude[18]), and diffusion coefficient (3 orders of magnitude[18]).

Petrenko[2] suggested that the ice subsurface layer may consist of several overlapping sublayers, each of which manifests in a different experiment. Thus, there may exist a sublayer of a density higher than that of ice which shows up in optical ellipsometry, a sublayer with high density of space charge contributing to the high surface conductivity of ice, a sublayer with partial disorder in the arrangement of water molecules which can be revealed in x-ray diffraction[27] or by proton-tunneling experiments,[28] and a sublayer with high-degree disorder in the hydrogen bond network,[27] and so forth. These layers may have different thickness and exist in different temperature intervals. Strong experimental support of this idea came recently from sophisticated X-ray diffraction experiments by Dosch *et al.*[27]

Recently, scanning force microscopy (SFM) was added to the impressive list of experimental techniques used to study ice surface and ice/solid interfaces.[13,14] The main attractiveness and potential advantage of the SFM is that it can combine near atomic spatial resolution with an ability to test *in situ* some physical properties, for instance, electrical conductivity, surface charge density, viscosity, and microhardness. Nevertheless, SFM is still very novel in the ice surface research, and several technical and theoretical problems must be solved before the technique becomes a powerful experimental tool in ice-surface and ice/solid-interface research. Some of these problems are addressed in the present paper.

Experimental Techniques

In all experiments described below, a commercial AutoProbe SA microscope with a 100-μm scanner (Park Scientific Instruments, Sunnyvale, California) was used for a contact scanning and acquisition of force curves (FC). Both high-voltage and low-voltage regimes of the scanner were used, depending on needed ranges of lateral and vertical scanning. To decrease the thermal power released in a piezolever we modified the scanner electronics. Namely, we decreased the DC bias applied to the piezolever from 1.25 to 0.116 V. This made the electric power

[⊗] Abstract published in *Advance ACS Abstracts,* July 15, 1997.

S1089-5647(96)03217-8 CCC: $14.00

distributed over the cantilever equal to 6.7 μwatt. An estimate similar to one made by Eastman *et al.*[23] showed that the temperature at the tip of the piezolever differed by less than 0.1 °C from the ambient temperature when our measurements were performed in air and by less than 0.01 °C when the piezolever was immersed in decane. To compensate for the decrease in sensitivity, we modified the scanner preamplifier, making its gain factor equal to 1000 instead of 100. The modified preamplifier significantly improved the signal-to-noise ratio.

We have used Si and Si_3N_4 (silicon nitride) piezolevers with spring constant of 2.5 N/m. The radius of the tip curvature R was measured using a Nb tip-calibration artifact (General Microdevices, Inc., Edmonton, AB, Canada). The value of R ranged from 30 to 120 nm for different tips.

We calibrated *z*-, *x*-, and *y*-detectors of the scanner once a week at each particular temperature used in the study. The possibility of pressure melting of the ice surface under the action of a tip will be discussed in the Experimental Results. Here it should just be noted that at $T \leq -1.5$ °C such melting has never occurred in our SFM tests, due to plastic relaxation of contact stress in ice.[22]

The scanner was enclosed in a sealed environmental chamber in which temperature and humidity were kept constant during the experiments. The temperature was maintained in the range from −0 to −20 °C with ±0.05 °C precision. High relative humidity (87 to 95 ± 2%) was maintained in the chamber to prevent rapid evaporation of the ice surface.

The environmental chamber had internal dimensions of 25 cm × 25 cm × 25 cm. A tiny "computer-chip" ventilator hung on four thin rubber strips and stirred air inside the chamber. The chamber was installed on a massive (60 kg) concrete platform and the latter hung from eight "tie-on," 4-ft long rubber strips, to minimize vibration from within the building generated by refrigeration system motors in the Ice Research Laboratory. The frame supporting the concrete platform and the environmental chamber on it was placed inside a large cold room in which we maintained the same temperature as in the chamber but with less precision (±0.5 °C). Work in the cold room permitted us to prepare, load, and change ice samples without exposing them to thermoshock and without deposition of frost micro crystals on the smooth ice surface. The microscope controller and computer were kept outside the cold room.

We used single crystals of ice grown from pure distilled, deionized, and degassed water. The water's specific resistivity was 18.3 MΩ cm. The ice crystals were grown using a fast growth technique[28] in which the water surface was cooled by intensive evaporation in a vacuum. As was obvious from large hexagonal figures on the upper surface of most of our crystals, their largest face coincided with a basal plane (0001). We double-checked the crystal orientation by placing the specimen between two crossed optical polarizers. In the process of developing of reliable technique we have tried to acquire FC and to scan ice specimens whose surface was prepared in several different ways: as grown in vacuum, flattened by a microtome machine, split by a scalpel, and first flattened by the microtome machine and then gently polished with an optically smooth and thoroughly cleaned quartz plane. All the surfaces were prepared in a cold room at $T = -10$ °C and then annealed at the same temperature during 2−4 h before SPM experiments were carried out on them. While the FCs obtained on all these types of samples were essentially similar, the scanning was most successful on the samples polished with the quartz plane. The other surfaces were too rough. Because of this all the results below refer to these kind of ice specimens.

The ice specimens had dimensions of 10 mm × 10 mm × 1 mm with the basal plane as their wider face. The samples were frozen at the bottom to a thick aluminum plate whose temperature was well controlled. When conductive Si cantilever tips were used, the potential difference between the tips and the electrically grounded ice samples was only 57 mV, with the "plus" on the cantilever tips.

In some experiments a drop of pure (for analysis) liquid decane was placed on the top of an ice sample, providing a (0.5−1.0)mm thick liquid film. Decane was chosen for its insolubility in water, its low freezing point, low vapor pressure, and low viscosity. In these experiments the piezolever and the ice surface were completely covered with decane.

Experimental Results

The general impression that one receives in studying the surface of ice on a microscopic scale and at temperatures above −20 °C is that the surface is very mobile, changeable, and tricky. This is especially true for the interface between ice and air. Even when the relative humidity is close to 100% and there is no appreciable temperature gradient, the microrelief on the ice surface permanently changes, and such a basic SFM procedure as the acquisition of force curves, when taken at different locations, may return different adhesion pull-off force values and a different liquid film thickness when measured at different moments of time.

Regarding these problems, SFM of the ice surface in decane has several advantages. First, a layer of decane prevents ice evaporation, thus making the ice surface much more stable. Second, the capillary forces between a liquid-like layer (when the layer is present) and a cantilever tip become very small and do not affect the microscope operations. In fact, in our experiments with cantilevers immersed in decane, the capillary forces were either absent or so small that we could not distinguish them from the electrical noise. Third, in decane the adhesion force applied to Si_3N_4 tips was absent or small. Typical force curves acquired in decane are shown in Figure 1a. We recorded such force curves (FC) at $T = -0.4$, -0.5, -0.6, -2.5, -10.8, -11.3, -15.5, and -20.0 °C and found a great deal of similarity at each of these temperatures. Note the smooth transition from the horizontal to the inclined part of the curve. At the very first contact between the cantilever tip and ice, force curves did not show this peculiar "roundness" but had a distinct corner located at the point of contact. Such a corner on the FC is characteristic of a tip touching a hard substrate. The "roundness" appeared on the FC only after several up-and-down cycles, and then the FC transformed into that shown in Figure 1a, became very reproducible, and showed no appreciable hysteresis. This behavior of the FCs was observed in the entire temperature range from −0.4 to −20.0 °C. The shape and dimensions of the "round" part of the FC vary little, if at all, with temperature (see also Figure 3). An interruption in the cycling for about 10 min restored the distinct corner on the first FC acquired after the interruption. Then the "roundness" reappeared.

Such a FC may be explained by either (1) noncontact repulsion between the tip and ice surface, or (2) the presence of a very soft but elastic layer on the ice. The "elastic" layer should exhibit nearly elastic behavior, since a hysteresis effect specific for plastic deformation does not exceed 5 nm in Figure 1a. We will show in the discussion section that 5 nm displacement corresponds approximately to plastic deformation of a *solid* ice surface under the pressure exerted by the tip. A thick (100 nm) liquid or liquid-like layer that does not wet the cantilever tip may behave like this, with surface tension playing

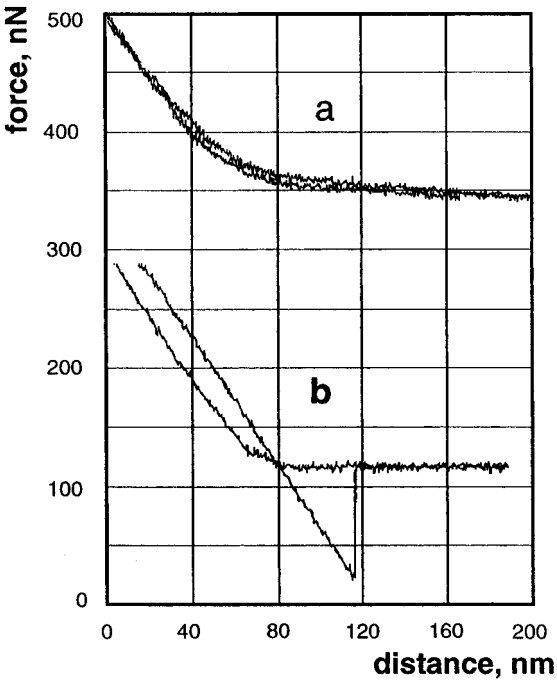

Figure 1. (a) Force curve taken on the (0001) face of an ice surface immersed in decane. A silicon nitride tip having a force constant of 2.5 N/m was used: the cycling frequency = 1 Hz, $T = -2.5$ °C. (b) Force curve taken on the (0001) face of an ice surface in air. A silicon nitride tip having a force constant of 2.5 N/m was used: the cycling frequency = 1 Hz, $T = -10.7$ °C, relative humidity = 89%.

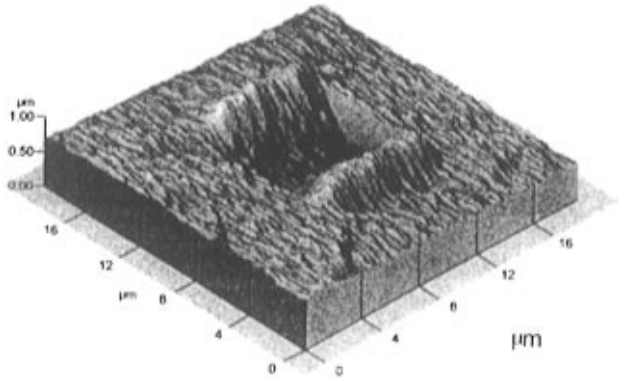

Figure 2. A well formed on the ice surface during the scanning procedure. Ice surface under decane, contact-mode scanning at $T = -20.0$ °C, set point = 50 nN, scanning frequency = 1 Hz, Si_3N_4 tip. The well depth is 0.22 μm, its width is 7.5 μm, and the banks' height = 0.23 μm.

the role of the elastic force. Nevertheless, it is extremely unlikely that the thickness of such a film would not depend on the temperature remaining almost constant between −0.4 and −20 °C. The pressure melting of ice has very strong temperature dependence[21] and vanishes at −22 °C. Moreover, Barnes *et al.*[22] showed that, under a wide variety of indentation times and in a wide temperature range, pressure melting does not occur due to relaxation of stress via fast plastic deformation. Interfacial premelting also has a very strong temperature dependence.[1]

Thus, the author believes that a noncontact repulsion between the ice surface and a dielectric-type tip was observed. Since this repulsion was also seen by us in air (notice the small "roundness" of the FC in figure 1b), van der Waals interaction cannot explain it because this interaction is always resulting in attraction not *repulsion.* Then we are left with an electrostatic repulsion as a single explanation of the observed noncontact interaction. It is important that we have not seen this repulsion

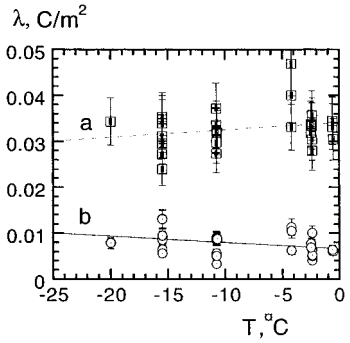

Figure 3. The surface charge density λ versus temperature calculated in the (a) elastic and (b) plastic approximations. Ice microhardness as a function of indentation time and temperature, found in ref 22, was used. Ice/(Si_3N_4-tip) interface in decane.

during very first approach of the tip to ice surface, and then it appeared and remained quite reproducible during a cyclic motion of the tip up and down. Hence this repulsion was produced by charge redistribution between the tip and ice surface. Generally, surface charges and surface double layers may cause a repulsion. We will discuss a likelihood of surface charges *versus* surface double-layers in the discussion section. On its first approach to the ice surface, the tip picks up a fraction of the surface charge, which causes mutual repulsion between tip and ice. Since decane is a good insulator, it takes a long time for the charges to decay. As was mentioned, a similar "roundness" of the force curves was also found in air (see Figure 1b), but due to the strong adhesion and capillary forces there was poor reproducibility of FC details when we worked in air. If we are interpreting correctly the FC shown in Figure 1a, then such FCs can be used to estimate the density of the surface charge on ice. This will be pursued further in the Discussion.

Studying the topography of the ice surface in decane, we found that even at such a low set point as 50 nN, a tip produced noticeable damage to the surface when the scanning area was small, see Figure 2. The larger the scanning area was, the smaller the damage was. At temperatures above approximately −14 °C, the damage produced by a small size scan disappeared before a larger scan was done. However, at −20 °C the lifetime of such wells was about 10 min. When a series of FCs is measured at the same location under low-temperature conditions (−20 °C), the tip creates a small shallow crater with a typical width of 2.5 μm and depth of 0.1−0.15 μm. We have not noticed such craters at higher temperatures, perhaps due to intensive "healing." Such healing is good evidence of intensive mass transport along the ice−decane interface for T above −14 °C.

As indicated above, it was much more difficult to use any contact mode of SFM to study the ice surface in air. The main obstacles were the strong adhesion and large capillary forces acting between the tips and a liquid-like layer. Adhesion and capillary forces were stronger for tips made of Si than those for silicon nitride tips. Most of our attempts to work with Si tips at temperatures above −4.5 °C resulted in ultimate capture of the tips by the ice surface and the loss of the tips. For Si tips, "necking," first found by Slaughterbeck *et al.*,[14] was typical. Another typical observation was time-dependent adhesion between Si tips and ice. At temperatures between −10 and −20 °C, the pull-off force increased in a consecutive series of FCs until the tip ultimately got stuck in the ice surface. On several occasions we observed stick-and-slip motion of a Si tip during a scanning procedure. That is, the tip was repeatedly captured by the ice surface and then released, thus moving in 50-nm "hops." The apparent height of the corresponding hops

due to tip bending was about 100 nm. Si-tip/ice-surface interaction is better explained in terms of ice growing on the tip. Then necking and adhesion occur between an ice specimen and ice on the tip. When a tip approached ice, we observed a sudden dip (jump-to-contact) of the tip toward the substrate (not shown in Figure 1 due to space limitation). This is evidence of a liquid or liquid-like layer on the ice surface.

Generally, reproducibility of FCs was poor when Si tips were used. We obtained more reproducible FCs with Si_3N_4 tips, see Figure 1b. Yet, even with these tips it was difficult to work in air above −4 °C. To determine the thickness d of the liquid-like layer, we carried out three series of FC measurements on three different ice samples at 14 different locations. All these measurements were carried out in air at −10.7 °C and RH = (90 ± 2)%. The magnitude of d was calculated as an amplitude of a jump-to-contact divided by a cantilever spring constant. Twelve results for d were grouped between 2 and 5 nm, while at two locations d was 13 and 16 nm. The average d calculated using the first 12 data points (excluding 13 and 16 nm) gave d = (3.45 ± 0.4) nm, where the error represent a standard deviation. We don't know the reason why d was not uniform along the ice surface. Note that an electrostatic attraction cannot explain the observed leaps of the tips to the ice surface because such an interaction first causes steadily increasing deflection of the tip and then a loss of cantilever stability, while we observed abrupt jumps of the tips to the ice. The measured pull-off force will be used in the Discussion to calculate ice/tip interfacial energy.

Discussion

Let us consider the physical processes that occur at the ice/tip interface during a routine scanning procedure and the acquisition of force curves. Namely, let us estimate the time it takes to establish thermal equilibrium between a tip and ice, magnitude of the elastic and plastic deformation, and the possibility of pressure melting. A clear understanding of these processes would enable us to interpret the experimental results described above.

In SFM experiments the tip either interacts with a small contact area πa^2 on the ice surface during limited time τ_{int} (FC mode) or the tip continuously changes its position (scanning mode). In the later case $\tau_{int} \approx a/\upsilon_{scan}$ where a is a radius of the contact area and υ_{scan} is a scanning velocity. We have to compare that time τ_{int} with time τ_{eq} it takes to establish thermal equilibrium in the point of the contact. If $\tau_{int} \gg \tau_{eq}$ then our experimental results refer to an ice/(tip's material interface). If $\tau_{int} \ll \tau_{eq}$, then the tip sees an ice/(ambient medium) interface as this interface was before the tip touched ice.

On the contact between a tip and ice a free energy of the system changes due to a change in the interfacial energy and/or due to possible melting of ice or refreezing of a LLL under the tip. Thus the contact point may behave either as a source or as a drain of heat. The time τ_{eq} that it takes to dissipate this heat through the ice, tip, and environment will mainly determine a rate with which the system approaches to equilibrium. Lattice dynamic transformation occur during much shorter time.

To estimate an upper limit for τ_{eq}, let us calculate the time it takes to dissipate the heat through ice only. Let us model a point of contact and the adjoining area (in which a phase transition may occur) with a hemisphere of radius R immersed in the ice surface. Let us now assume an instantaneous change of heat quantity ΔQ inside the hemisphere. The characteristic time in which the system attains a thermal equilibrium can be estimated as

$$\tau = \frac{\Delta Q}{\dot{Q}} \approx \frac{C_V \Delta T \frac{4\pi R^3}{3}}{4\pi R^2 \chi \frac{dT}{dR}} \approx \frac{C_V R^2}{3\chi} \approx 3ns \qquad (1)$$

where C_V is ice thermal capacity (1.89×10^6 J/m^{3}K), R = 100 nm, and χ is ice thermal conductivity (2 wt/m K). In eq 1 we estimated dT/dR as $\Delta T/R$. A precise solution of a similar problem (a sphere in an infinite medium[20]) gives the relaxation time $C_V R^2/4\chi$. Thus, our simple approximation works well.

In our SFM experiments, τ_{int} exceeded 50 μs in scanning mode and 50 ms in FC mode. Thus, $\tau_{int} \gg \tau_{eq}$ and we always tested properties of ice/(tip material) interfaces. For this reason we will not discuss neither the ice/air nor ice/decane interfaces.

Two other critical parameters that we have to calculate are the contact area between the tip and the ice s and the pressure generated by the tip P. Let us estimate the size of the contact area using the JKR theory.[26] In this theory two elastic spheres of radii R_1 and R_2, will flatten together under an external load of force, F, such that their contact area will have a radius a.

$$a = \left\{\frac{R}{k}[F + 3\pi RW + \sqrt{6\pi RWF + (3\pi RW)^2}\right\}^{1/3} \qquad (2)$$

where R is the reduced radius, $R = R_1R_2/(R_1 + R_2)$ and k is the effective Young's modulus. In our case R is the tip radius of about 100 nm, k = 9.5 Gpa, and W is the work of adhesion.

Let us consider a Si_3N_4 tip with an end radius R = 100 nm. Let the tip be attached to a cantilever having 2.5 N/m spring constant. A typical force acting on the tip in a scanning regime was from −50 to +50 nN, and in the FC regime the force typically varied from −100 to 200 nN. We used the temperature range from −0.4 to −20 °C, and the indentation time (for the FC) varied from 50 ms to 12.5 s. Equation 2 implies a purely elastic interaction between the tip and the ice. When W = 0, a = 7.9 and 12.6 nm for F = 50 and 200 nN, respectively. In the case of W = 0.1 J/m^2, a = 14 and 17.2 nm for F = 50 and 200 nN, respectively. Thus, the first conclusion we can make is that the contact area is much smaller than the tip radius: $a \ll R$. Let us compare this result with the one predicted by a plastic approximation. When W = 0,

$$a = \sqrt{\frac{F}{\pi H}} \qquad (3)$$

where H is the microhardness of ice. Using $H = 6 \times 10^7$ N/m^2 (−10 °C, loading time = 1 s[27]), we will have a = 17 and 33 nm for F = 50 and 200 nN, respectively. Here again, $a \ll R$. Now let us estimate the pressure generated by the tip. In the elastic approximation, P = 80 MPa (W = 0.1 J/m^2, F = 50 nN) and P = 214 MPa (W = 0.1 J/m^2, F = 200 nm). From the phase diagram of water the depression of the ice melting point ΔT due to pressure P is expressed as

$$T \approx (7.4 \times 10^{-8}\ °C/Pa) \times P \qquad (4)$$

This predicts ΔT = 5.9 °C for F = 50 nN and ΔT = 15.8 °C for F = 200 nN. Fortunately, the pressure, and hence ΔT, reduces dramatically due to the plastic deformation of ice under the tip. Barnes et al.[22] measured ice hardness H in a wide range of temperature, 0− −25 °C, and loading time, 0.1 ms to 10^4 s. They showed that, due to ice ductility, the pressure melting of ice does not take place at temperatures below −1.5 °C. For us, it means that pressure melting may affect the results only at −0.4, −0.5, and −0.6 °C. Also important is the finding by Barnes *et al.* that at T = −2 °C the pressure generated by an

indenter is reduced due to the plastic deformation even during very short time equal or shorter than 0.1 ms. Thus, the plastic approximation conditions were always present when we used a tip−ice interaction time from 50 msec to 12.5 s and worked at $T \leq -2.5$ °C.

Finally, the plastic approximation predicts an indentation depth, z, equal to 1.3 nm ($F = 50$ nN) and 5.4 nm ($F = 200$ nN). Thus, one can expect that the hysteresis due to the plastic deformation of ice should not exceed approximately 5 nm.

The pull-off force shown in Figure 1b can be used to estimate an interfacial energy of ice/Si_3N_4 interface when that interface is "dry", *i.e.*, does not include a LLL, or F can be used to estimate a capillary pressure when a LLL separates the solid ice and the tip.

While we have a good evidence for LLL in ice/air interface (the jump-to-contact at $T > -13$ °C) we have not seen such evidence when ice was covered with liquid decane. Eastman and Zhu[23] suggested that, when there is a liquid-like layer between ice and a tip, the latter should immerse continuously into the ice after a contact with ice surface. We did not observed that kind of force curves.

In air the pull-off force F is proportional to an interfacial energy:[24,25]

$$F = -4\pi R\gamma_{sv} \tag{5}$$

where γ_{sv} is the ice/Si_3N_4 interfacial energy. Substitution of the typical pull-off force observed at $T = -10$ °C and $F = (100 \pm 15)$ nN gives $\gamma_{sv} \approx (80 \pm 12)$ mJ/m^2, where the error represents a standard deviation calculated for 25 FCs. As an alternative explanation, notice that capillary pressure generated by a thin liquid-like layer should give a contribution of

$$F = -4\pi R\gamma_{LLL}\cos\theta \tag{6}$$

where γ_{LLL} is the surface tension of the liquid-like layer and θ is the contact angle between the liquid-like layer and Si_3N_4.[30] We do not know the value of γ_{LLL}, but a substitution of that of water at 0 °C, 75 mJ/m^2, or the surface energy of an ice/vapor interface $\gamma_{iv} \approx 109$ mJ/m^2 [21] for γ_{LLL} would give a pull-off force quite similar to that shown in Figure 1b (if $\cos\theta \approx 1$). This similarity might be either an indirect evidence for LLL or accidental. For the case of Si tips in which the pull-off forces were much larger and grew with time we may assume either that R was larger, due to the ice coating the tip, and/or that there was a larger Si/ice interfacial energy.

Finally, since we know now that $a \ll R$ and $z \ll R$, we can calculate the surface charge density that would account for the observed repulsion force seen in Figure 1a. The electrostatic repulsive force between two parallel disks of radius a and surface charge density λ

$$F_{rep} = \frac{\pi a^2\lambda^2}{2\epsilon\epsilon_0} \tag{7}$$

will be at a maximum when the distance between the tip and the ice is much less than a. In eq 7, λ is assumed to be equal on the tip and on the ice and ϵ is a dielectric constant of decane. We calculated λ from the maximum repulsive force using both the elastic and plastic approximations discussed above to determine a; thus found λ is shown in Figure 3. The error bars in this figure correspond to an error in determination of the maximum repulsive force just before a direct contact between a tip and ice, *i.e.*, the point at which the straight line (Hook's law) intersects with the round part of the FCs. On the basis of the Barnes *et al*. results, we believe more the plastic approximation that yields $\lambda \approx 10^{-2}$ C/m^2. If the *microhardness* measured by them was less than *nanohardness* in our experiments, then λ should be somewhat between one given by the elastic and plastic approximations.

Note that within the data scattering λ does not depend on temperature. The magnitude of $\lambda \approx 10^{-2}$ C/m^2 is of the same order of magnitude as the one calculated by Kroes[14] for a free ice surface and it also is similar to that found as an upper limit of the surface charge density estimated using frictional electrification of ice[31] and that estimated by Dosch *et al.*[27] Surface density of D-defects that would account for such large λ is 3×10^{-2} defect/ surface site. Simple estimates showed that to explain 100 nN repulsion force acting between two double-layers of radius a (17 to 33 nm) one has to assume that the occupancy of surface sites by D-defects exceeds 1, and this is not realistic.

Summary

In this paper we studied the interactions between ice surface and microcantilever tips made of Si and Si_3N_4. The main questions we addressed were (1) What is the kind of physical processes occur during dynamic ice/tip interaction? (2) Is a thermal equilibrium maintained during the scanning and acquisition of force curves? (3) Do the SFM data refer to an ice/(tip material) or ice/(ambient medium) interfaces? (4) What kind of quantitative information can be obtained from such SFM experiments?

First, our analysis showed that pressure melting of ice under the tip does not normally occur below −1.5 °C. Second, the thermal equilibrium between a tip and ice always take place even in the faster scanning mode. Because of this SFM study of ice provide information on the properties of ice/(tip material) interfaces.

When FC's were acquired in air at $T > -13$ °C a LLL manifested in the jump-to-contact motion of the tip. The layer thickness was estimated as (3.5±0.4)nm at $T = -10.6$ °C and RH = 90%.

It was also found that the ice surface and a Si_3N_4 tip begin to repulse each other after first few consecutive contacts. The quantitative analysis of the data favors an electrostatic interaction between two like charges sitting on the tip and ice surface as an explanation of this repulsion. The corresponding charge density is about 10^{-2} C/m^2.

At temperatures above −14 °C, a rapid healing of ice−surface damages induced by the tip was found in decane. This phenomenon evidences an intensive mass transport in the ice subsurface layer and can be used in future to study this transport quantitatively.

Acknowledgment. This research is supported by the ARO under Grant DAAH04-95-1-0189. It was also supported in part by the NSF under Grant DMR-9413362 and by the ONR under Grant N00014-95-1-0621. The author thanks Dr. Samuel Fain for fruitful discussions of the results and of their interpretation.

References and Notes

(1) Dash, J. G., Fu, H. and Wettlaufer, J. S. *Rep. Prog. Phys.* **1995**, *58* (1), 115.

(2) Petrenko, V. F. (1994a) *The Surface of Ice*; U.S. Army CRREL Special Report No. 94-22; U.S. Army Cold Regions Research and Engineering Laboratory, Corps of Engineers, Department of the Army, U.S. Department of Defense: Hanover, NH, 1994.

(3) Furukawa, Y.; Ishikawa, I. *J. Cryst. Growth* **1993**, *128*, 1137.

(4) Beaglehole, D.; Wilson, P. *J. Phys. Chem.* **1994**, *98*, 8096.

(5) Barer, S. S.; Kvlividze, V. I.; Kurzaev, A. B.; Sobolev, V. D.; Churaev, N. V. *Dokl. Akad. Nauk* **1977**, *235*, (3), 601.

(6) Sonwalkar, N.; Shyam Sunder, S.; Sharma, S. K. *Appl. Spectrosc.* **1993**, *47*, 1585.

(7) Chrazanowski, J. J. *Mater. Sci. Lett.* **1988**, *7*, 1058.

(8) Jellinek, H. H. G. *J. Colloid Sci.* **1959**, *14*, 268.
(9) Gilpin, R. R. *J. Coll. Interface Sci.* **1980**, *77*, 435.
(10) Maruyama, M., Bienfait, M., Dash, J. G.; Coddens, G. *J. Cryst. Growth* **1992**, *118*, 33.
(11) Fu, H. Y.; Dash, J. G. *J. Coll. Interface Sci.* **1993**, *159*, 343.
(12) Landy, M.; Freiberger, A. *J Coll. Interface Sci.* **1967**, *25*, 231.
(13) Nickolayev, O.; Petrenko, V. *MRS Symposium Proceedings*; Demczyk, B. G., *et al.*, Eds.; MRS: Pittsburgh, 1995; Vol. 355, p 221.
(14) Slaughterbeck, C. R.; Kukes, E. W.; Pittenger, B.; Cook, D. J.; Williams, P. C.; Eden, V. L.; Fain, S. C. *J. Vac. Sci. Technol. A* **1996** *14* (3), *1213*.
(15) Dzyaloshinskii, I. E.; Lifshitz, E. M.; Pitaevskii, L. P. *Adv. Phys.* **1961**, *10*, 165.
(16) Elbaum, M.; Schick, M. *Phys. Rev. Lett.* **1991**, *66* (13), 1713.
(17) Wilen, L. A.; Wettlaufer, J. S.; Elbaum, M.; Schick, M. *Phys. Rev. B.* **1995**, *52*, 12426.
(18) Mizuno, Y.; Hanafuza. N. *J. Phys. C1.* **1987**, *48* (3), 511.
(19) Dash, J. G. *Frost Heave and the Surface Melting of Ice. Phase Transitions in Surface Films 2*; Taub, H., *et al.*, Eds.; Plenum Press: New York, 1991; p 339.
(20) Carslaw, H. S.; Jaeger, J. C. *Conduction of Heat in Solids*; Clarendon Press: Oxford, **1959**; p 294.
(21) Hobbs, P .V. *Ice Physics*; Clarendon Press: Oxford, 1974; Chapter 6.
(22) Barns, P.; Tabor, D.; Walker, J. C. F. *Proc. R. Soc.*, London **1971**, *A324*, 127.
(23) Eastman, T.; Da-Ming-Zhu. *J. Colloid Interface Sci.* **1995**, *172*, 297.
(24) Derjaguin, B. V. *Kolloid—Z.* **1934**, *69*, 155.
(25) Israelashvili, J. *Intermolecular and Surface Forces;* Academic Press: London, 1991; Chapter 15.
(26) Johnson, K. L.; Kendall, K.; Roberts, A. D. *Proc. R. Soc., London* **1971**, *A324*, 301.
(27) Dosch, H., Lied, A.; Bilgram, J. H. *Surf. Sci.* **1996**, *366*, 43.
(28) Golecki, I.; Jaccard, C. *J. Phys. C: Solid State Physics* **1978**, *11*, 4229.
(29) Khusnatdinov, N. N.; Petrenko, N. N. *J. Cryst. Growth* **1996**, *163*, 420.
(30) Kroes, G. J. *Surf. Sci.* **1992**, *275*, 365.
(31) Petrenko, V. F.; Colbeck, S. C. *J. Appl. Phys.* **1995**, *77*, 4518.